

Research Article

Influence of Different Tapered Implants on Stress and Strain Distribution in Bone and Implant: A Finite Element Analysis

Bijan Heidari¹ • Hossein Bisadi² • Behnam Heidari³ • Mahdi Kadkhodazadeh^{4*}

¹Assistant Professor, Department of Prosthodontics, Dental School, Hamadan University of Medical Sciences, Hamadan, Iran

²Assistant Professor, Department of Mechanical Engineering, Iran University of Science and Technology, Tehran, Iran

³Mechanical Engineer, Hamadan, Iran

⁴Assistant Professor, Department of Periodontics, Dental School, Hamadan University of Medical Sciences, Hamadan, Iran

*Corresponding Author; E-mail: shayad1358@yahoo.com

Received: 15 August 2009; Accepted: 1 September 2009; Published online: 11 October 2009

J Periodontol Implant Dent 2009; 1(1):11-19 (2009e2)

This article is available from: <http://dentistry.tbzmed.ac.ir/jpid>

© 2009 The Authors; Tabriz University of Medical Sciences

This is an Open Access article distributed under the terms of the Creative Commons Attribution License (<http://creativecommons.org/licenses/by/3.0>), which permits unrestricted use, distribution, and reproduction in any medium, provided the original work is properly cited.

Abstract

Background and aims. Finite elemental analysis is an efficient technique for investigating biomechanical interactions of different implant designs. The purpose of this study was to investigate the effect of cylindrical and tapered implants with different degree of tapering and similar lengths on the stress and strain distribution in the bone and implant.

Materials and methods. One cylindrical and five types of tapered implants with degrees of tapering from 0.02 to 0.16 were modeled to this study. The implant material was grade IV titanium and abutment was grade ELI titanium. The bone model used comprised of compact and spongy bone assumed to be homogeneous, isotropic and linearly elastic.

Results. With increased degree of implant tapering, the von Mises stress and strain increased in the bone. However, at the neck of implant, the most sensitive area, with increase in degree of tapering, both stress concentration and strain decreased. The lowest stress and strain were generated in the most tapered implant.

Conclusion. Based on the results, cylindrical screw implant generated the lowest maximum von Mises stress in cortical bone and tapered implant type 5 with highest taper degree generated the highest maximum von Mises stress.

Key words: Biomechanics, dental implants, finite element analysis, stress distribution.

Introduction

Treatment planning for oral rehabilitation is nowadays mostly based on using dental implants, the function of which are transferring loads to the surrounding biological tissue. Although long-term clinical studies report 95% survival for mandibular and 65% to 85% survival for maxillary implants, failure may result

from loss of osseointegration or component failure subsequent to restoration and may be related to unfavorable loading or to high stress concentrations.¹ There are more than 90 dental implant body designs available. Biomechanical rationale of dental implant designs may evaluate these designs as to their efficacy to many biomechanical loads.² Review of literature shows different implant survival rates and different

marginal bone loss for various implant body designs.³⁻¹³

Dental implants have macroscopic and microscopic design components. Variation in component design among implant systems may lead to different stress/strain distribution, thus altering the transmission of forces to surrounding bone.¹⁴ Smooth-sided, cylindrical and tapered implants have a component of compressive load to be delivered to the implant-bone interface, depending on the degree of taper.¹⁵ However, there are limitations for the amount of implant tapering.²

Finite elemental analysis (FEA) is an efficient technique for investigating biomechanical interactions of different implant designs. Numerous studies have been performed to assess force distribution following load application to implants of various dimensions.^{4,5,16-18}

To enhance clinical success, it is necessary to understand how the stress concentration on implants is affected by the shape, width, and height of thread. The use of the finite element method (FEM) in implant biomechanics analysis offers many advantages over other methods in simulating the complexity of clinical situations.¹⁵

The aim of this study was to determine the effect of different tapered implants (with different gradient in bone and similar vertical length) and cylindrical screw on the stress and strain distribution in bone and implant.

Materials and Methods

Implants and abutments were designed and then analyzed with Ansys version 10 computer software (Swanson, Washington, USA). Because the models were symmetric to a plane as well as axis-symmetric (as shown in Figure 1), we designed two-dimensional models.

Compact and spongy bone were assumed to be

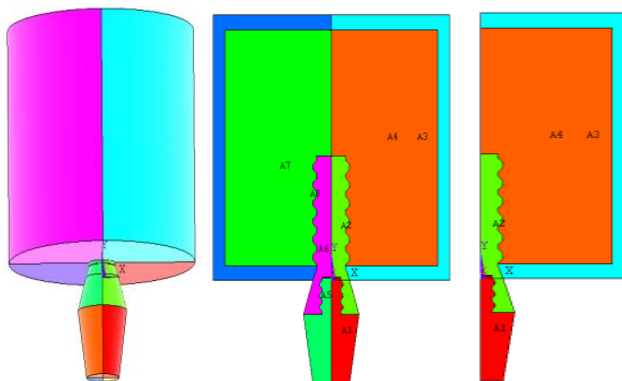


Figure1. Models are symmetric to a plane and are axis-symmetric.

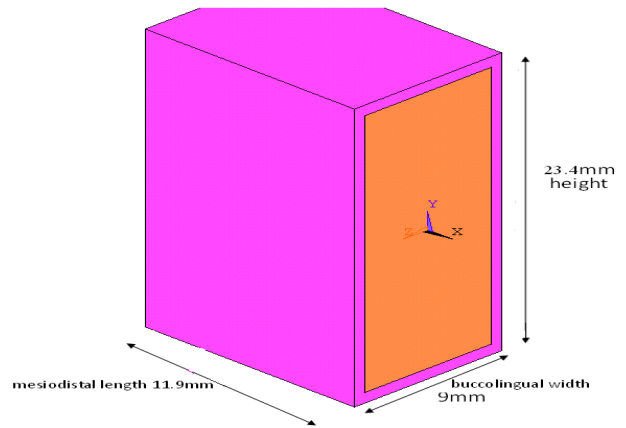


Figure 2. Bone dimension.

homogeneous, isotropic and linearly elastic. The thickness of the compact bone layer in the model was assumed to be 1.3 mm as shown in Figure 2. The overall dimensions of the bone were 23.4 mm in height, 23.8 mm in mesiodistal length and 9 mm in buccolingual width. The material properties used in the finite element analysis are shown in Table 1.

Five tapered dental implants with tapering degree of 0.02, 0.06, 0.1, 0.12, and 0.16; and one cylindrical implant with similar length (13.6 mm) and diameter (4 mm) were used; the abutment height was 6 mm. Implant pitch for all implants used is shown in Figure 3. No thread was modeled at the cortical bone level.

All materials used in the models were considered to be, homogenous, isotropic and linearly elastic. The implant material was titanium grade IV and abutment was titanium grade ELI. For the titanium implant and titanium abutment, elastic module of 114 GPa and 113.8 GPa, and for compact bone and spongy bone, elastic module of 14 Gpa and 1.5 Gpa were used.

Meshing and loading

Because of its symmetry, only half of the model was meshed with plane 83 elements, and 0.02 mm distance between implant and abutment was meshed by contact element using contact manager. This is the most important stage of meshing. Obviously, use of different elements and also distinct condition at the interface of

Table 1. The material properties used in the finite element analysis

Material	Elastic module (GPa)	Poison ratio
Titanium grade ELI (abutment)	114	.38
Titanium grade IV (implant)	113.8	.34
Cortical bone	14	.3
Spongy bone	1.5	.3

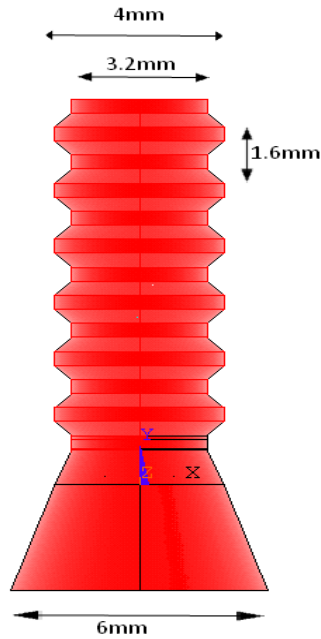


Figure 3. Implant dimension.

implant and abutment causes different results in stress and strain.

Meshing consisted of 2861 elements and 8299 nodes Figures 4a & 4b. The two-dimensional models were constrained in all directions at the nodes on the upper edge and in direction on the right boundary. Important to the symmetry in the model is boundary condition (BC) symmetry on left boundary. Finally, a pressure of 30 psi, which is close to normal occlusal pressure, was applied axially on lower edge of the abutment Figure 5.

Results

Stress/strain distribution in bone

As shown in Figures 6 and 7, in all types of implants assessed, von Mises stress distribution in the bone was similar; however, maximum von Mises stress increased as implants were more tapered. In all types of implants, maximum von Mises stress occurred in a region of cortical bone adjacent to implant neck and lower bound of cortical bone. The highest maximum stress was generated in tapered implant type 5 (0.572 MPa, Figure 7b).

Maximum von Mises strain was generated in the spongy bone. Strain distributions in all types of implant in spongy bone were similar, with a slight increase as implants were more tapered. Maximum strain was seen in the apex of implant in the spongy bone Figure 8. With only 30 psi auxiliary pressure, Maximum von Mises strain was observed in type 5 tapered implant (strain 0.11×10^{-3} , Figure 9b). Results of stress and strain distribution are shown in Table 2 and maximum

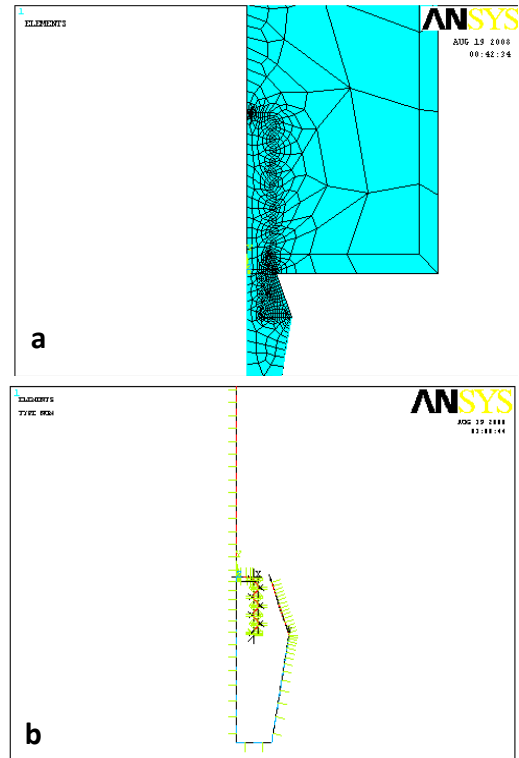


Figure 4. Meshing with plane 83 elements (a) and using contact element between implant and abutment (b).

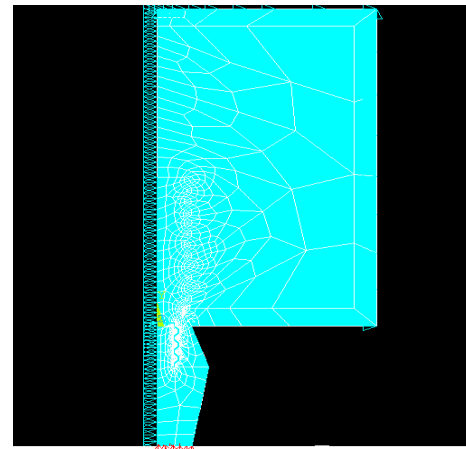


Figure 5. Boundary condition symmetry on left boulder of model and using 30 psi on lower edge of abutment.

von Mises stress and strain in bone are plotted in Figures 10a and 10b.

Table 2. Maximum von Mises stress and strain in bone for all types of implant under 30 psi auxiliary pressure

Implant type	Maximum von Mises stress (MPa)	Maximum von Mises stress ($\times 10^{-4}$)
Cylindrical	.466	.881
Conic 1	.475	.850
Conic 2	.500	.941
Conic 3	.523	.981
Conic 4	.538	1
Conic 5	.572	1.1

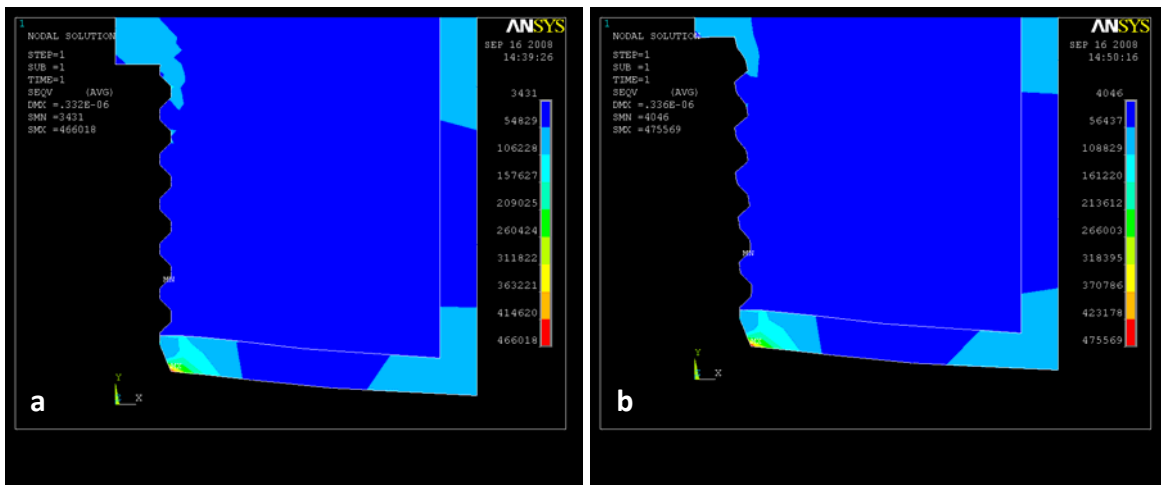


Figure 6. von Mises stress distribution in the cylindrical type from 3431 Pa to 466118 Pa (a) and conic type 1 with 0.2 gradient from 4040 Pa to 475569 Pa (b).

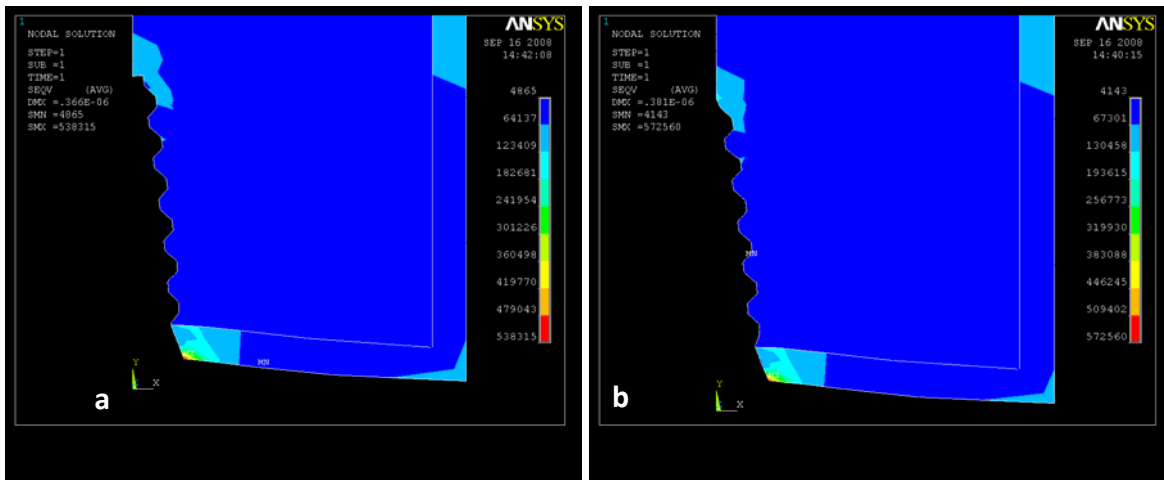


Figure 7. von Mises stress distribution in the conic type 4 with 0.12 gradient from 4865 Pa to 538315 Pa (a) and conic type 5 with 0.16 gradient from 4143 Pa to 572560 Pa; highest max stress is generated in this type (b).

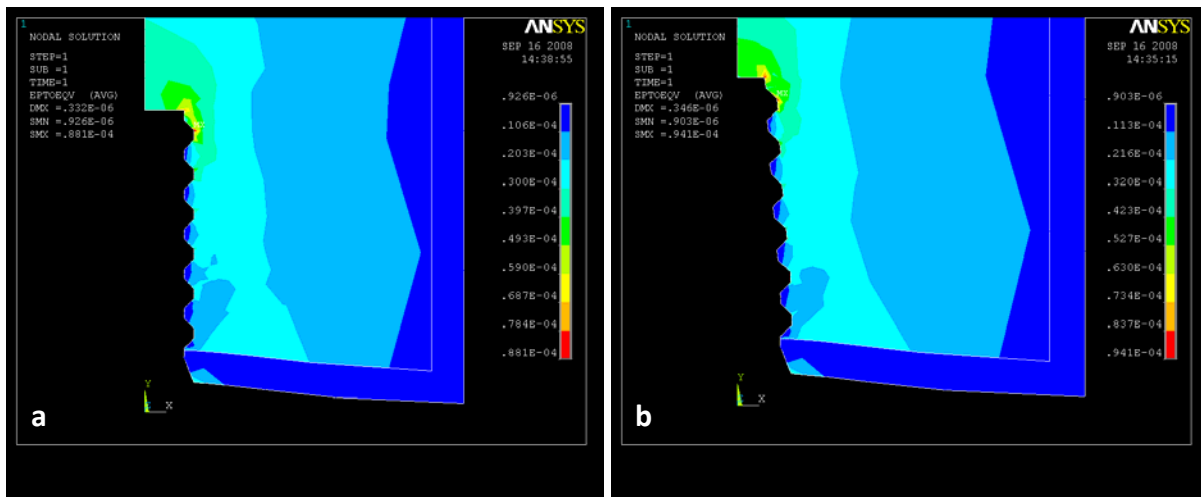


Figure 8. von Mises strain distribution in the cylindrical from 0.926×10^{-6} to 0.881×10^{-4} Pa (a) and conic type 2 with 0.06 gradient from 0.903×10^{-6} to 941×10^{-4} a Pa (b).

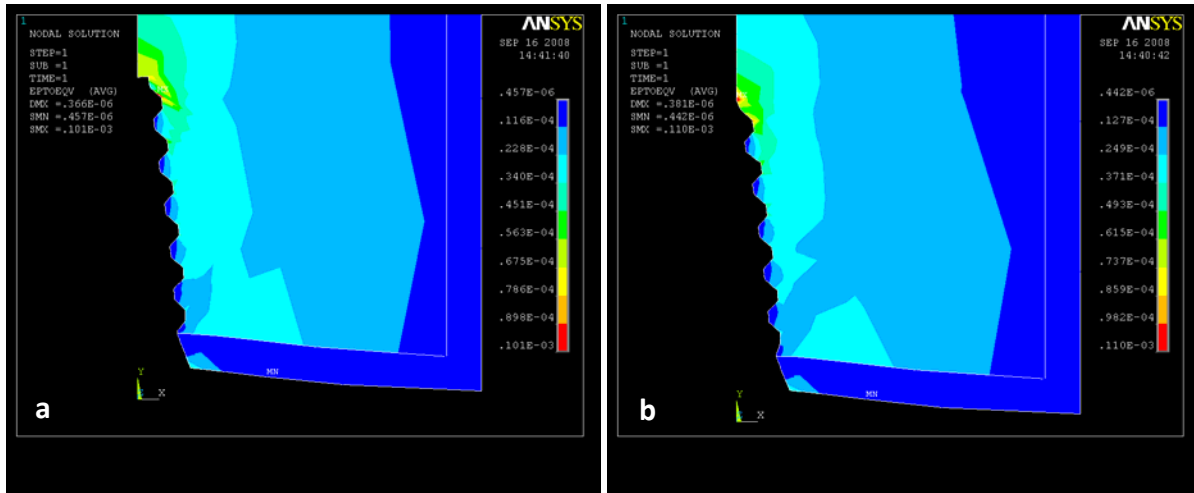


Figure 9. von Mises strain distribution in the conic type 4 with 0.12 gradient from $.457 \times 10^{-6}$ to $.101 \times 10^{-3}$ Pa (a) and conic type 5 with 0.16 gradient from $.442 \times 10^{-6}$ to $.110 \times 10^{-4}$ Pa; highest max strain is generated in this type (b).

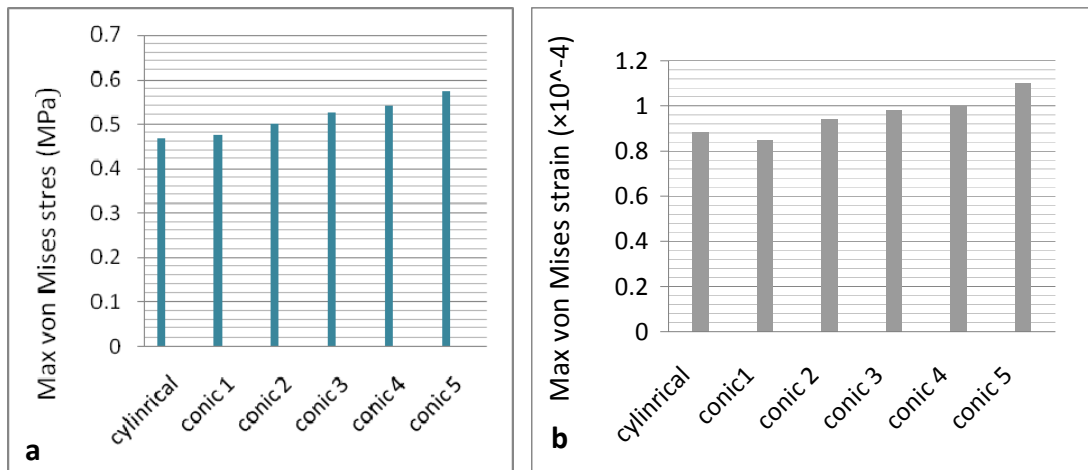


Figure 10. Maximum von Mises stress (a) and strain (b) in all bones under 30 psi axial pressure.

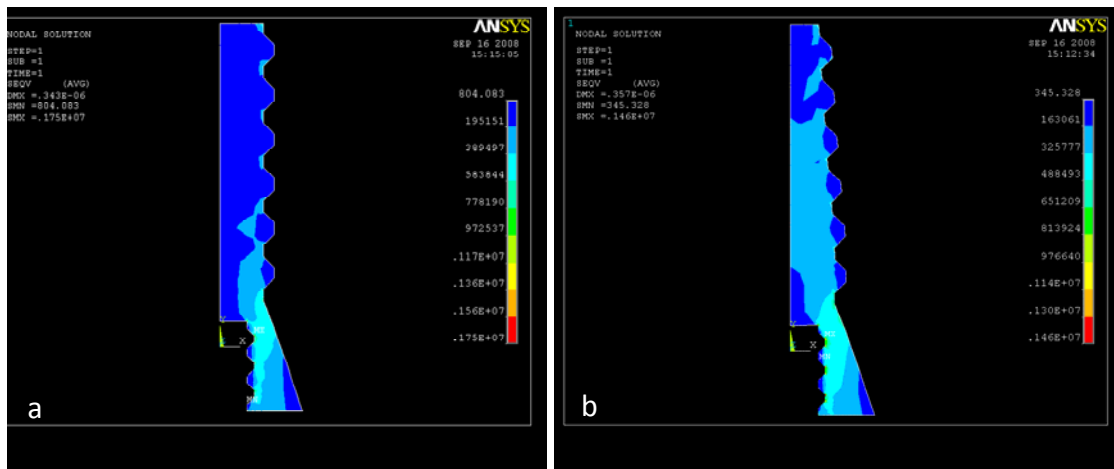


Figure 11. von Mises stress distribution in the cylindrical type from 804 to $.175 \times 10^7$ Pa (a) and conic type 2 with 0.06 gradient from 345 to $.146 \times 10^7$ Pa; lowest maximum stress is generated in this type (b).

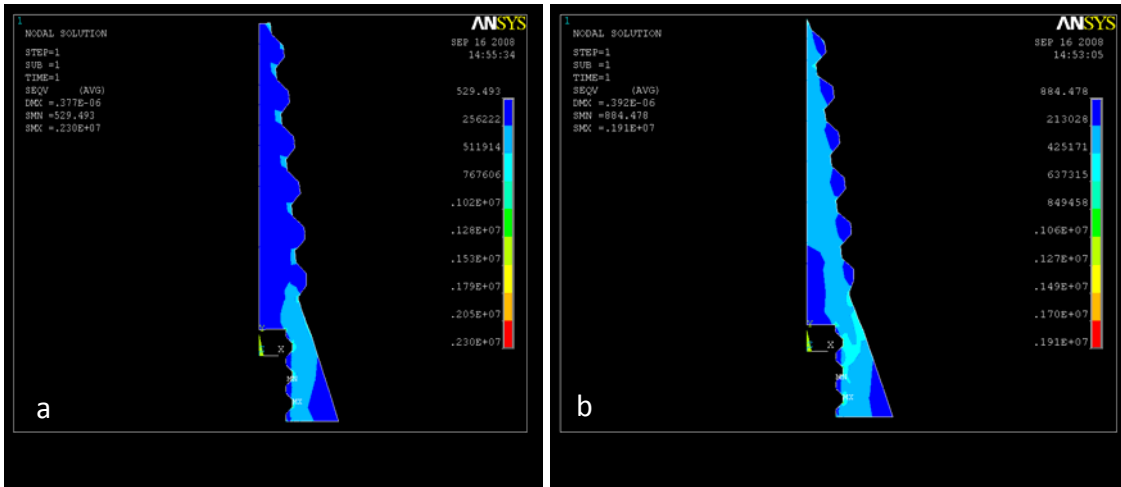


Figure 12. von Mises stress distribution in the conic type 4 with 0.12 gradient from 529.5 to $.23 \times 10^7$ Pa, the highest max stress is generated at this type (a) and conic type 5 with 0.06 gradient from 884 to $.191 \times 10^7$ Pa (b).

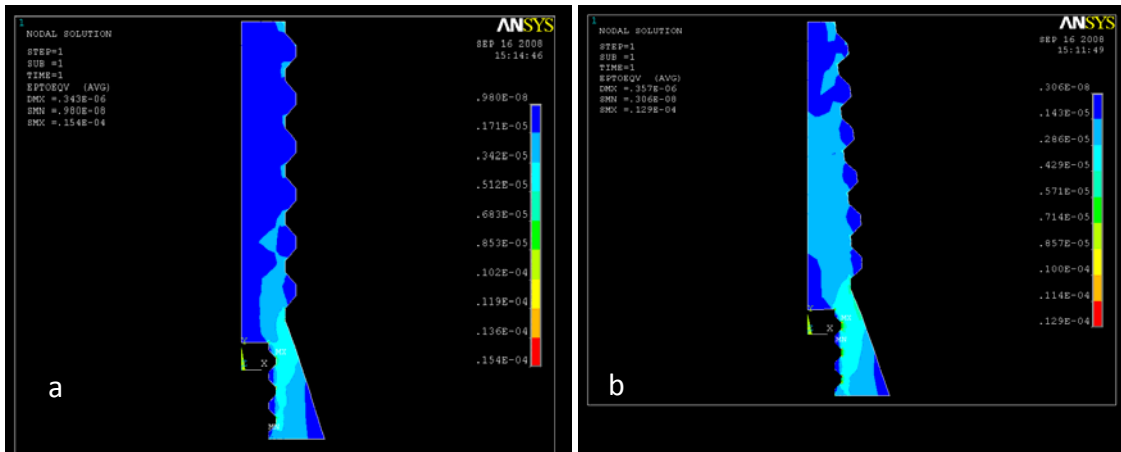


Figure 13. von Mises strain distribution in the cylindrical type $.98 \times 10^{-8}$ to $.154 \times 10^{-4}$ Pa (a) and conic type 2 with 0.06 gradient from $.306 \times 10^{-8}$ to $.129 \times 10^{-4}$ Pa; lowest maximum strain is generated in this type (b).

Stress/strain distribution in implant

As shown in Figures 11 and 12, in all types of implant-maximum stress was generated at the abutment-implant interface. The lowest maximum stress was generated in tapered implant type 2 (Figure 11b), and the highest maximum stress was generated in type 4 tapered implant (Figure 12b). It is, however, important to note that from type 1 to type 4, stress concentration decreased at the neck of implant in the region between cortical bone and abutment. At this region, in implant type1, stress was 0.38 to 0.58 MPa; however, in type 4, stress at the same region was 0.25 to 0.5 MPa. For all implants, stress distribution gradually increased from neck to apex; however, in tapered implant type 4, stress concentration decreased intensely at the neck, which seems like an area of restricted stress distribution.

A different pattern was observed with strain, as the only similarity of all types of implants was in that max strain was generated at the abutment-implant interface.

The lowest maximum strain was generated in tapered implant type 2 (0.129×10^{-4} , Figure 13b) and the highest was generated in tapered implant type 4 (0.202×10^{-4} , Figure 14b). Table 3 summarizes the results of maximum stress and strain for all implant types evaluated. Charts of maximum von Mises stress and strain are plotted in Figures 15a & 15b.

Discussion

Although implant failures are still unavoidable, the successful use of dental implants has been well docu-

Table 3. Maximum von Mises stress and strain for all types of implants under 30 psi axial pressure

Implant type	Maximum von Mises stress (MPa)	Maximum von Mises strain ($\times 10^{-4}$)
Cylindrical	1.75	.154
Conic 1	1.8	.165
Conic 2	1.46	.129
Conic 3	1.54	.135
Conic 4	2.3	.202
Conic 5	1.91	.168

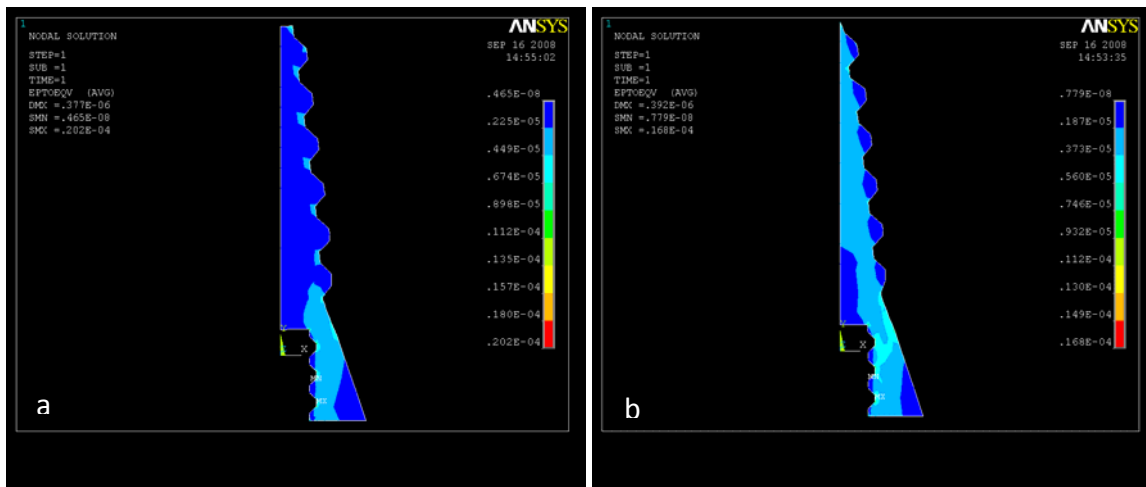


Figure 14. von Mises strain distribution in conic type 4 with 0.12 gradient from $.465 \times 10^{-8}$ to $.202 \times 10^{-4}$ Pa; the highest max stress is generated in this type (a); and conic type 5 with 0.16 gradient from 0.779×10^{-8} to 0.168×10^{-4} Pa (b).

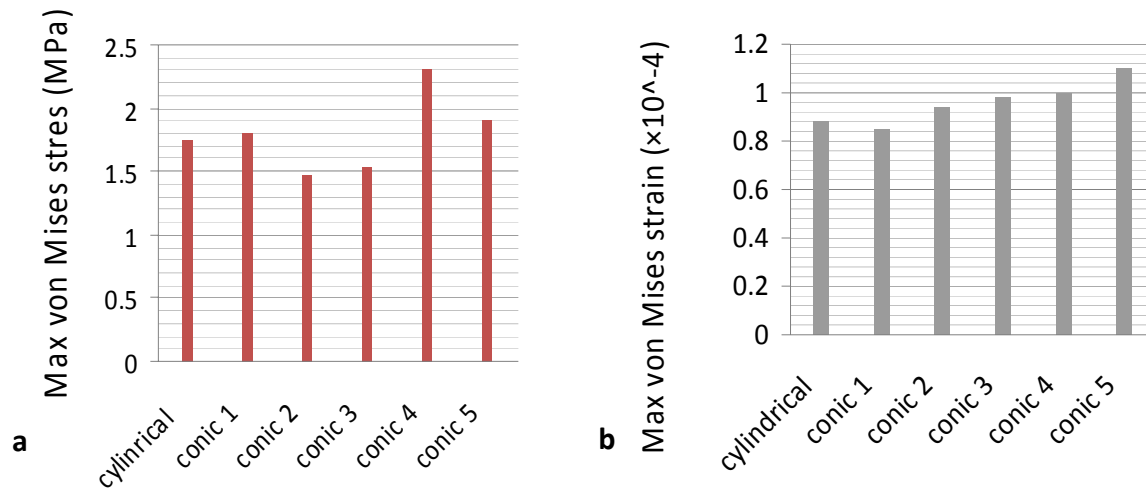


Figure 15. Maximum von mises stress (a) and strain (b) in all types of implants under 30 psi axial pressure.

mented.¹⁹⁻²¹ The mechanisms responsible for implant failure are not fully understood, owing to complications from many related factors, such as loading condition, prosthesis type, implant design, implant position, bone type, and material properties of the bone-implant interface.¹

Dental implant failure may result from loss of osseointegration or component failure subsequent to restoration and may be related to unfavorable loading or to high stress concentrations.¹⁹⁻²² Bone quality is also an important factor, with more failures found in low quality of bone.¹⁹⁻²³ These factors are difficult to investigate clinically, because of limited information as well as sample variation.

Variations in design among dental implant systems may lead to different stress/strain distributions, thus altering the transmission of forces to surrounding

bone.²⁴⁻²⁶ In the case of osseointegrated dental implants, occlusal loads are transmitted directly to the surrounding bone. However, in natural teeth, the periodontal ligament acts as an intermediate cushion element to buffer occlusal forces.

Several studies have attempted to minimize crestal bone resorption by increasing the bone-implant contact and, therefore, decreasing stress at the alveolar crest.⁶⁻¹² To enhance clinical success, it is necessary to understand how the stress concentration on implants is affected by the shape, width, and height of thread. The use of the finite element method in implant biomechanics analysis offers many advantages over other methods in simulating the complexity of clinical situations.¹⁵

Pierrisnard et al⁵ performed a finite element analysis of 3.75-mm-wide hex-headed screw-type implants of 6

to 12 mm in length and reported that the magnitude and distribution of stress to the bone was constant and independent of implant length. These findings were contradicted by Petrie & Williams,⁵ who performed a finite element analysis of implants with diameters of 3.5 to 6 mm and lengths of 5.75 to 23.5 mm, placed in molar regions, and reported a reduction in peak crestal stress following force application with implants of increasing diameter and/or length. In contrast, Holmgren et al⁵ and Himmlova et al⁵ demonstrated that force application resulted in greatest force concentration at the bone crest and that implant length had no effect on either the magnitude of peak stress or stress distribution to the supporting bone. The preponderance of finite element analyses demonstrates that implant length has no effect on the magnitude of stress experienced by the supporting alveolar bone crest around implants, which would seem to support the use of shorter implants if they offer specific advantages in given clinical situations.⁵

The generation of high stress distribution or concentration in the bone should be avoided to achieve stable osseointegration for implant restoration; therefore, the influence of implant on stress and strain distribution in the bone must be investigated. In this study, the effect of implant on stress distribution in the bone under vertical pressure was investigated by performing finite element analysis using Ansys computer software with contact friction at the interface between the abutment and implants. Six types of implant, one cylindrical and five tapered, with similar vertical lengths and different degrees of tapering were selected. Maximum von Mises stress in the bone occurred at the region of cortical bone adjacent to implant neck and lower bound of cortical bone.

In the present study, maximum von Mises stress occurred at the implant-abutment interface for all implants. Maximum stress was registered at the crestal bone, which is the most sensitive area. With increase in the degree of tapering, stress concentration decreased. In cortical bone as the degree of tapering increased, the maximum von Mises stress and strain also increased; therefore, the maximum von Mises is generated in tapered implant type 5 with 0.16 tapering. The highest maximum von Mises stress and strain was generated in tapered implant type 4 with 0.12 degree tapering and the lowest maximum von Mises stress and strain was seen in tapered implant type 2 with 0.06 degree tapering.

Conclusion

Based on the results of the analyses, it was found that cylindrical screw implant generated the lowest maxi-

mum von Mises stress in cortical bone and tapered implant type 5 with highest tapering generated the highest maximum von Mises stress, probably because of reduced and sharper surface area.

References

1. Lin CL, Wang JC, Ramp LC, Liu PR. Biomechanical response of implant systems placed in the maxillary posterior region under various conditions of angulation, bone density, and loading. *Int J Oral Maxillofac Implants* 2008;23:57-64.
2. Misch C, Strong T, Bidez MW. Scientific rationale for dental implant design. In: Misch C, ed. *Contemporary Implants Dentistry*, 3rd ed. St Louis: Mosby; 2008: 203-4.
3. Kao HC, Gung YW, Chung TF, Hsu ML. The influence of abutment angulation on micromotion level for immediately loaded dental implants: a 3-D finite element analysis. *Int J Oral Maxillofac Implants* 2008;23:623-30.
4. Las Casas EB, Ferreira PC, Cimini CA Jr, Toledo EM, Barra LP, Cruz M. Comparative 3D finite element stress analysis of straight and angled wedge-shaped implant designs. *Int J Oral Maxillofac Implants* 2008;23:215-25.
5. Fugazzotto PA. Shorter implants in clinical practice: rationale and treatment results. *Int J Oral Maxillofac Implants* 2008;23:487-96.
6. Matsushita Y, Kitoh M, Mizuta K, Ikeda H, Suetsugu T. Two-dimensional FEM analysis of hydroxyapatite implants: diameter effects on stress distribution. *J Oral Implantol* 1990;16:6-11..
7. Meijer HJ, Kuiper JH, Starmans FJ, Bosman F. Stress distribution around dental implants: influence of superstructure, length of implants, and height of mandible. *J Prosthet Dent* 1992;68:96-102.
8. Palmer RM, Smith BJ, Palmer PJ, Floyd PD. A prospective study of Astra single tooth implants. *Clin Oral Implants Res* 1997;8:173-9.
9. Holmgren EP, Seckinger RJ, Kilgren LM, Mante F. Evaluating parameters of osseointegrated dental implants using finite element analysis--a two-dimensional comparative study examining the effects of implant diameter, implant shape, and load direction. *J Oral Implantol* 1998;24:80-8.
10. Nordin T, Jönsson G, Nelvig P, Rasmusson L. The use of a conical fixture design for fixed partial prostheses. A preliminary report. *Clin Oral Implants Res* 1998;9:343-7.
11. Norton MR. Marginal bone levels at single tooth implants with a conical fixture design. The influence of surface macro- and microstructure. *Clin Oral Implants Res* 1998;9:91-9.
12. Chun HJ, Cheong SY, Han JH, Heo SJ, Chung JP, Rhyu IC, et al. Evaluation of design parameters of osseointegrated dental implants using finite element analysis. *J Oral Rehabil* 2002;29:565-74.
13. Tada S, Stegaroiu R, Kitamura E, Miyakawa O, Kusakari H. Influence of implant design and bone quality on stress/strain distribution in bone around implants: a 3-dimensional finite element analysis. *Int J Oral Maxillofac Implants* 2003;18:357-68.
14. Geramy A, Morgano SM. Finite element analysis of three designs of an implant-supported molar crown. *J Prosthet Dent* 2004;92:434-40.
15. Kong L, Hu K, Li D, Song Y, Yang J, Wu Z, Liu B. Evaluation of the cylinder implant thread height and width: a 3-dimensional finite element analysis. *Int J Oral Maxillofac Implants* 2008;23:65-74.
16. Sevimay M, Turhan F, Kiliçarslan MA, Eskitascioglu G. Three-dimensional finite element analysis of the effect of different

- bone quality on stress distribution in an implant-supported crown. *J Prosthet Dent* 2005;93:227-34.
17. Yokoyama S, Wakabayashi N, Shiota M, Ohyama T. Stress analysis in edentulous mandibular bone supporting implant-retained 1-piece or multiple superstructures. *Int J Oral Maxillofac Implants* 2005;20:578-83.
 18. Lin CL, Hsu KW, Wu CH. Multi-factorial retainer design analysis of posterior resin-bonded fixed partial dentures: a finite element study. *J Dent* 2005;33:711-20.
 19. Sahin S, Cehreli MC, Yalçin E. The influence of functional forces on the biomechanics of implant-supported prostheses—a review. *J Dent* 2002;30:271-82.
 20. Cehreli M, Sahin S, Akça K. Role of mechanical environment and implant design on bone tissue differentiation: current knowledge and future contexts. *J Dent* 2004;32:123-32.
 21. Gross M, Laufer BZ. Splinting osseointegrated implants and natural teeth in rehabilitation of partially edentulous patients. Part I: Laboratory and clinical studies. *J Oral Rehabil* 1997;24:863-70.
 22. Becker CM, Kaiser DA, Jones JD. Guidelines for splinting implants. *J Prosthet Dent* 2000;84:210-4.
 23. Martinez H, Davarpanah M, Missika P, Celletti R, Lazzara R. Optimal implant stabilization in low density bone. *Clin Oral Implants Res* 2001;12:423-32.
 24. Holmes DC, Loftus JT. Influence of bone quality on stress distribution for endosseous implants. *J Oral Implantol* 1997;23:104-11.
 25. Adell R, Lekholm U, Rockler B, Brånemark PI. A 15-year study of osseointegrated implants in the treatment of the edentulous jaw. *Int J Oral Surg* 1981;10:387-416
 26. Haas R, Polak C, Furhauser R, Mailath-Pokorny G, Dortbudak O, Watzek G. A long-term follow-up of 76 Brånemark single-tooth implants. *Clin Oral Implants Res* 2002;13: 38-43.